

Article

Analysis of the Insulation Characteristics of Hexafluorobutene (C₄H₂F₆) Gas and Mixture with CO₂/N₂ as an Alternative to SF₆ for Medium-Voltage Applications

Rizwan Ahmed ¹, Rahisham Abd Rahman ^{1,*}, Adel S. Aldosary ², Baqer Al-Ramadan ², Rahmat Ullah ³
and Arshad Jamal ⁴

- ¹ Faculty of Electrical and Electronic Engineering, University Tun Hussein Onn Malaysia, Batu Pahat 86400, Malaysia; rizwan.ciit016@gmail.com
- ² Architecture and City Design Department, King Fahd University of Petroleum & Minerals, Box #684, Dhahran 31261, KFUPM, Saudi Arabia
- ³ Advanced High Voltage Engineering Research Center, School of Engineering Cardiff University, Cardiff CF10 3AT, UK
- ⁴ Transportation and Traffic Engineering Department, Imam Abdulrahman Bin Faisal University, Dammam 34211, Saudi Arabia
- * Correspondence: rahisham@uthm.edu.my

Abstract: This paper investigates C₄H₂F₆, a promising environmentally friendly insulating gas that possesses high dielectric strength and a low global warming potential. The study focuses on examining the insulation properties of C₄H₂F₆ when combined with CO₂/N₂, aiming to assess its suitability as a substitute for SF₆ in gas-insulated applications. Finite element analyses are performed to evaluate the field utilization factor and electric field distribution in the proposed mixture. The properties of liquefaction temperature were examined in this study to determine the optimal mixing ratio for applications that require a minimum working temperature. Extensive experimental investigations were carried out to assess the dielectric strength characteristics of the gas mixture in both uniform and quasi-uniform electric fields. It was found that pure HFO-1336mzz (E) exhibits a dielectric strength approximately 1.2–1.6 times higher than SF₆. Experimental results have revealed that the insulation performance of a 30% HFO-1336mzz (E)/CO₂ mixture closely resembles that of SF₆, with a matching efficiency of up to 90% in a weakly uniform electric field. This remarkable performance can be attributed to a positive synergistic effect between HFO-1336mzz (E) and CO₂, combined with the gas mixture's excellent self-recoverability property. These experimental findings are further supported by finite element analysis, which confirms the observed results. The 30% HFO-1336mzz (E)/CO₂ gas mixture at 0.15–0.20 MPa pressure and constant 0.6 mm air gap reveal superior insulation tolerance and less sensitivity to the electric field, confirming its promising medium-voltage engineering applications. The associated results of this research provide a critical reference for the engineering application of the alternating (AC) and direct current (DC) insulation characteristics of the HFO-1336mzz (E)/CO₂ gas mixture.

Keywords: global warming potential; dielectric strength; SF₆; gas insulation; eco-friendly gases



Citation: Ahmed, R.; Rahman, R.A.; Aldosary, A.S.; Al-Ramadan, B.; Ullah, R.; Jamal, A. Analysis of the Insulation Characteristics of Hexafluorobutene (C₄H₂F₆) Gas and Mixture with CO₂/N₂ as an Alternative to SF₆ for Medium-Voltage Applications. *Appl. Sci.* **2023**, *13*, 8940. <https://doi.org/10.3390/app13158940>

Academic Editors: Qiuqin Sun, Haoxi Cong and Feng Bin

Received: 4 July 2023

Revised: 31 July 2023

Accepted: 2 August 2023

Published: 3 August 2023



Copyright: © 2023 by the authors. Licensee MDPI, Basel, Switzerland. This article is an open access article distributed under the terms and conditions of the Creative Commons Attribution (CC BY) license (<https://creativecommons.org/licenses/by/4.0/>).

1. Introduction

Sulfur hexafluoride (SF₆) is extensively employed in high-voltage gas-insulated equipment (GIE) due to its high dielectric strength, excellent arc interruption performance, and low boiling point. However, SF₆ is a strong greenhouse gas with a global warming potential (GWP) 23,500 times that of CO₂ [1]. There has been a 20% rise in the amount of SF₆ in the atmosphere over the last five years, and it is estimated that 80% of the SF₆ generated globally is utilized in the power sector [2,3]. Reducing SF₆ emissions now might add 1.5% to the Paris agreement's aim of maintaining the global average temperature increase to far

below 2 °C [4]. SF₆ was one of the six primary greenhouse gases included in the Kyoto Protocol in 1997 [5,6]. This makes it imperative to work on decreasing or capping SF₆ use. The pursuit of a gas insulation medium that may substitute SF₆ as safely as possible has gained significant attention in recent years. Therefore, the realization of SF₆-free practices has now become a crucial task for the green development of power grids.

Many studies have been carried out throughout the years on the insulating capacities of several gases as SF₆ substitutes [7–9]. No gas or gas mixture has been found to this day which can completely replace SF₆. Hence, gases that can replace SF₆ must have (1) outstanding physicochemical properties, such as a low liquefaction temperature, low toxicity, good thermal and chemical stability, and non-flammability; (2) exceptional insulation and arc quenching abilities; and (3) excellent environmental characteristics, specifically low GWP and Ozone Depletion Potential (ODP) values [10]. ODP is defined as “Relative amount of degradation caused to the ozone layer compared with trichlorofluoromethane (R-11 or CFC-11) being fixed at an ODP of 1”.

Two types of alternatives to SF₆ were investigated: naturally occurring buffers and synthetic gases. Buffer gases include natural gases (CO₂, N₂, and dry air) [11–13], and synthetic gases include gases such as PFCs, CF₃I, and *c*-C₄F₈ [14,17]. The use of buffer gases such as carbon dioxide as a dielectric medium requires large equipment due to momentous expansion in pressure. Moreover, 100% CO₂ insulation characteristics are only around 40% of SF₆. Although carbon dioxide’s safety and low cost are advantageous factors, implementing it in practical medium-voltage applications would require replacing the existing equipment with bulky construction to sustain high pressure to provide sufficient dielectric strength. Synergistic effects allow for a decrease in GWP proportional to the admixture ratio in SF₆-based gas mixtures like SF₆/N₂ and SF₆/CF₄ while maintaining usable electric characteristics [12]. Tetrafluoropropene, a novel chemical with four interesting properties, was only discovered recently [13]. It was determined that fluoroketones (C₅-FK) [14], fluoronitriles (C₄F₇N) [15], and trifluoroiodomethane [16] have sufficient electric strength to be employed in electrical equipment under realistic working circumstances. They are usually mixed with low-boiling-point gases, such as carbon dioxide (CO₂) or nitrogen (N₂), when utilized in HV applications because of their high boiling points. The new alternatives have an electric strength comparable to SF₆ and a reduced GWP. Despite the fact that the aforementioned new ecologically friendly insulation gases have been researched and suggested, none of them are a satisfactory substitute because they all have drawbacks. For example, the biological toxicity of C₄F₇N is still debatable, and its GWP is very high (about 2400). The high liquefaction temperature of C₅F₁₀O limits its practical applications since it requires too much buffer gas. Lastly, HFO-1234ze (E) and HFO-1336mzz (Z) were the HFO gases suggested as insulating medium. HFO-1234ze (E) has a lower insulating strength than SF₆ and a lower liquefaction temperature (−19.4 °C at 0.1 MPa) [17]. The dielectric strength of HFO-1336mzz (Z) is twice that of SF₆, but it has a very high boiling point of 33.4 °C [18].

In this paper, we suggest transhexafluoro-2-butene (HFO-1336mzz (E)/(C₄H₂F₆)) as a promising dielectric gas. HFO-1336mzz (E) is a common refrigerant because it has good thermal stability, is colorless, and has no fire or explosion risks. HFO-1336mzz (E) has a very short atmospheric lifespan (days to weeks) and a low GWP of just approximately 18. Since no chlorine nor bromine is present, the ODP value is 0. Because its molecules have such strong electronegative characteristics, they provide a great insulating performance, 1.2 to 1.4 times higher than benchmark SF₆. HFO-1336mzz (E) has the drawback of a high liquefaction temperature, about 8 °C, limiting its application as a dielectric gas. To compensate for the drawback of its high boiling point, the proposed gas should be mixed with a buffer gas, such as N₂ or CO₂, with temperatures of −196 °C and −79 °C, respectively [19].

Related investigations on the insulation capabilities of HFO-1336mzz (E) are currently lacking. Rabie et al. 2015 executed computational screening of several insulating gases, and among them, HFO-1336mzz (E)’s dielectric characteristics were estimated to be almost

1.8 times those of SF₆ [20]. Kothe et al. 2020 tested a number of new environmentally beneficial gases. They discovered that the insulating strength of HFO-1336mzz (E) and CO₂ or N₂ is comparable to that of mixtures of C₅F₁₀O/CO₂ and C₄F₇N/CO₂ [21]. Its synergistic interactions with various buffer gases and its breakdown characteristics in inhomogeneous electric fields remain unknown. The molecular structure and chemical properties of HFO-1336mzz (E) gas are shown in Figure 1 and Table 1, respectively.

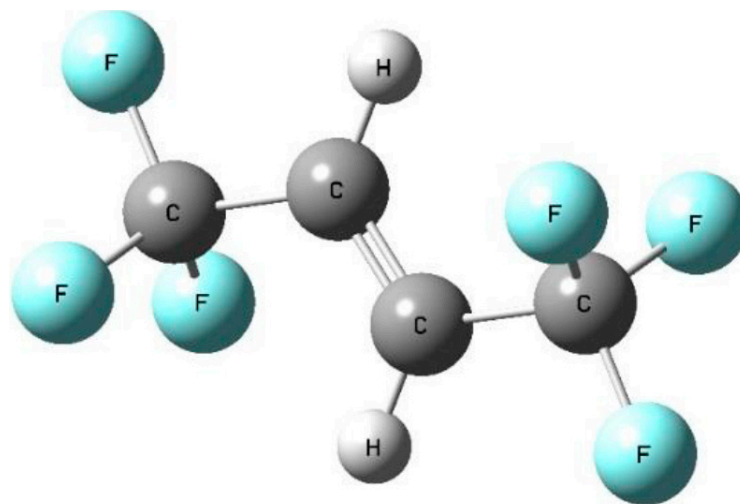


Figure 1. Chemical structure of C₄H₂F₆ or HFO-1336mzz (E).

Table 1. Basic physical and chemical properties of HFO-1336mzz (E), SF₆, CO₂, and N₂.

Parameters	SF ₆	HFO-1336mzz (E)	CO ₂	N ₂
Cas no	2551-62-4	66711-86-2	124-38-9	1179900-47-0
Chemical formulae	SF ₆	C ₄ H ₂ F ₆	CO ₂	N ₂
GWP	23,500	18	1–3	265–298
ODP	0	0	0	0
Boiling point	−63.9 °C	7.5 °C	−79.0 °C	−195.8 °C
Melting point	−51 °C	−20 °C	−78.5 °C	−210 °C
Critical temperature	45.60 °C	137.7 °C	31.1 °C	−146.9 °C
Critical pressure	37.64 bar	3.15 bar	73.8 bar	33.9 bar
Molecular mass (g/mol)	146.05	164.5	44.01	14.01
Flammability	None	None	None	none
Odor/Color	Odorless/Colorless	Odorless/Colorless	Odorless/Colorless	Odorless/Colorless
Stability	Stable	Stable	Stable storage condition	Stable storage condition
Solubility in water	Trace	0.280 g/L at 25 °C	Relatively low solubility	Relatively low solubility

2. Materials and Methods

This research work is divided into two phases, finite element modeling and insulation strength testing. HFO-1336mzz (E) and the mixture's dielectric breakdown strength were investigated under HVAC and HVDC conditions. The experiments were conducted following the IEC60270 standard, and standard atmospheric conditions were maintained in the lab (temperature $t_0 = 20$ °C, pressure $b_0 = 0.1013$ MPa, absolute humidity $h_0 = 11$ gm/m³) [22]. The TERCO test setup generates HVAC and HVDC test voltages for experiments. The test vessel is modified to meet the technical requirement of changing the electrode's air gap. For this purpose, a linear actuator is installed at the bottom layer of the test vessel. The test vessel is composed of aluminum, and plexiglass is used as the vessel window. The vessel height is 800 mm, the width is 90 mm, and the thickness of the vessel wall is 5 mm. Hence, based on the dimensions, the total volume of the test gas is approximately 5 L and can bear a pressure of 0.6 MPa. A constant electrode gap distance of 6 mm is maintained throughout the experimental and simulation analysis. Pressure and vacuum gauges are

installed to accurately measure the gas pressure inside the vessel. A one-way air valve is installed at the bottom flange to pump gas from the vessel in and out. Prior to conducting the experiments, the test chamber was vacuumed to 0.09 MPa through a vacuum pump and then filled with CO₂. This process is repeated 5 times to ensure no impurities are left inside the pressure vessel.

Gas breakdown occurs as the critical field strength is achieved, and the externally applied voltage is recorded as the breakdown voltage. To investigate the basic insulation performance, i.e., the electric strength near its intrinsic strength, weakly non-uniform and uniform fields are used. These field distributions are formed by plane–plane and sphere–plane electrode configurations. The advantages of a sphere–plane arrangement are a simplified alignment, a relatively compact size, and fast conditioning due to the small surface area stressed by the highest field. The sphere–plane arrangement can create field utilization factors representing real GIS and representing real GIS components such as switches. A plane–plane electrode arrangement’s main advantage is the uniformity of field distribution [23].

The electrode configurations are plane–plane and sphere–plane for uniform and slightly uniform electric fields. All the electrodes are cleansed with anhydrous alcohol and dried with cotton to remove the dust. The electrode surfaces are polished with 5000 mesh sandpaper to ensure that the surface roughness value is below 2.5 μm; as a further precaution, 3 aging tests are conducted on the test electrode configuration before every test to remove the protuberances and tiny particles on the electrodes. The electrode schematic diagram can be seen in Figure 2. An AC voltage of known value is applied to the buffer gas CO₂ to calibrate and validate the measuring apparatus’s accuracy. The test gas HFO1336-mzz (E) and buffer gases are injected into the pressure vessel following Dalton’s law of partial pressure. A standing time of 24 h is provided to ensure gas mixture uniformity. Considering the insulation medium’s recovery time, the interval between two adjacent breakdowns was set to three minutes. A slow voltage increase rate avoids overestimations of the electric strength due to the statistical time lag but increases the experimental time. Therefore, a fast voltage ramping rate is utilized up to around 80% to 90% of the expected breakdown voltage, and then the voltage is increased in small steps of 0.5 kV/s compared to the initial breakdown value. Under each test condition, at least ten repeated tests were performed. If the initial and consecutive breakdown voltage error is greater than 10%, the test will be repeated, and then the test’s average value is recorded as the breakdown voltage. Moreover, benchmark tests are also conducted using pure SF₆ gas.

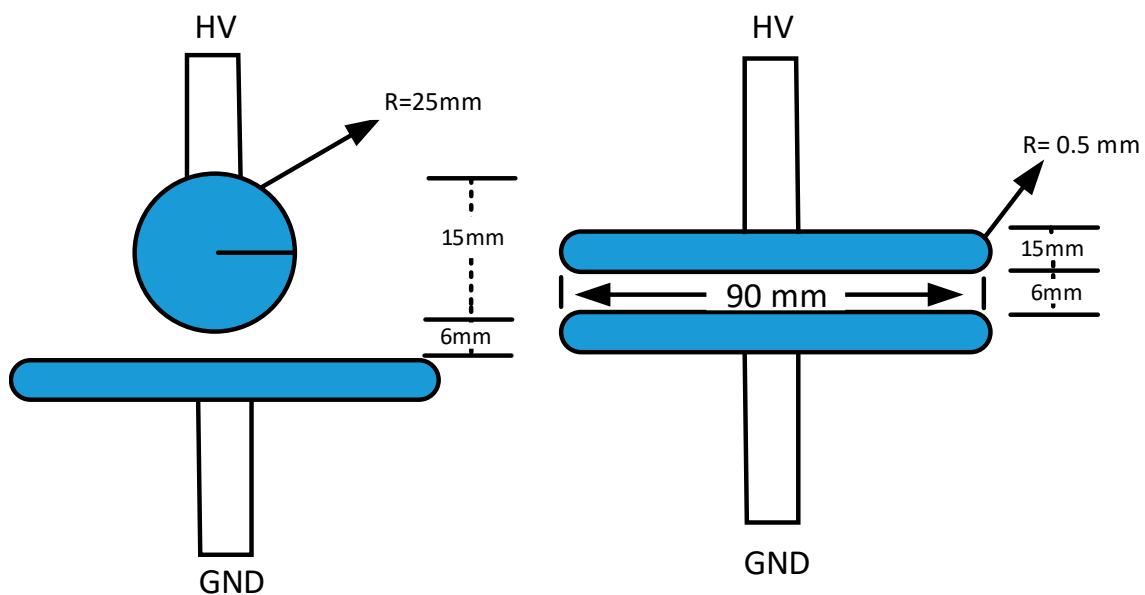


Figure 2. Electrode setup and geometry.

3. Experimental Setup

The experiment circuit is presented in Figures 3 and 4 for HVAC and HVDC, respectively. IEC60270 [24] is the basis for the experimentation procedure. A control desk (HV 9103) includes a peak, impulse, and DC voltmeter and a variable voltage supply. The control desk operates and controls the HVAC, HVDC, and impulse equipment. The supply voltage to HV9103 is 220–230 V, 50 Hz, and the regulating voltage is 0–220 V AC. During HVAC breakdown, a resistor (HV9121) is attached to safeguard the test transformer (HV 9105), which has an output of 220 V–100 kV in a single stage and 200 kV in two stages. The breakdown voltage is measured in real time by the voltmeter via a measuring capacitor (HV9141), as shown in Figure 3. The HVDC voltage up to 140 kV, 50 mA, and 50 Hz is generated via an experimental setup, as shown in Figure 4. The circuit consists of two HV rectifiers (HV9111) connected with a control desk (HV9103) and a smoothing capacitor (HV9112). A measuring resistor HV9113 measures the DC breakdown voltage. All the equipment can discharge itself except the smoothing capacitor, which is discharged through an external earthing switch.

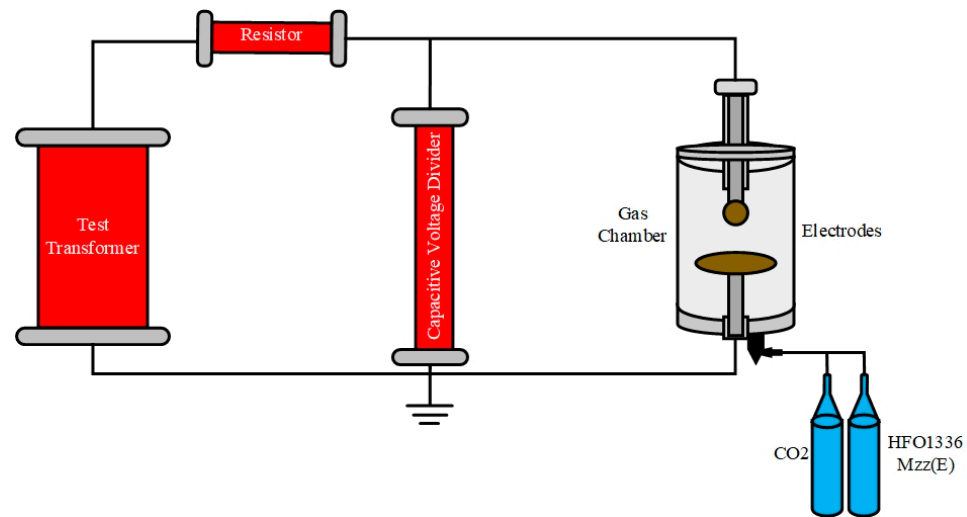


Figure 3. HVAC test setup.

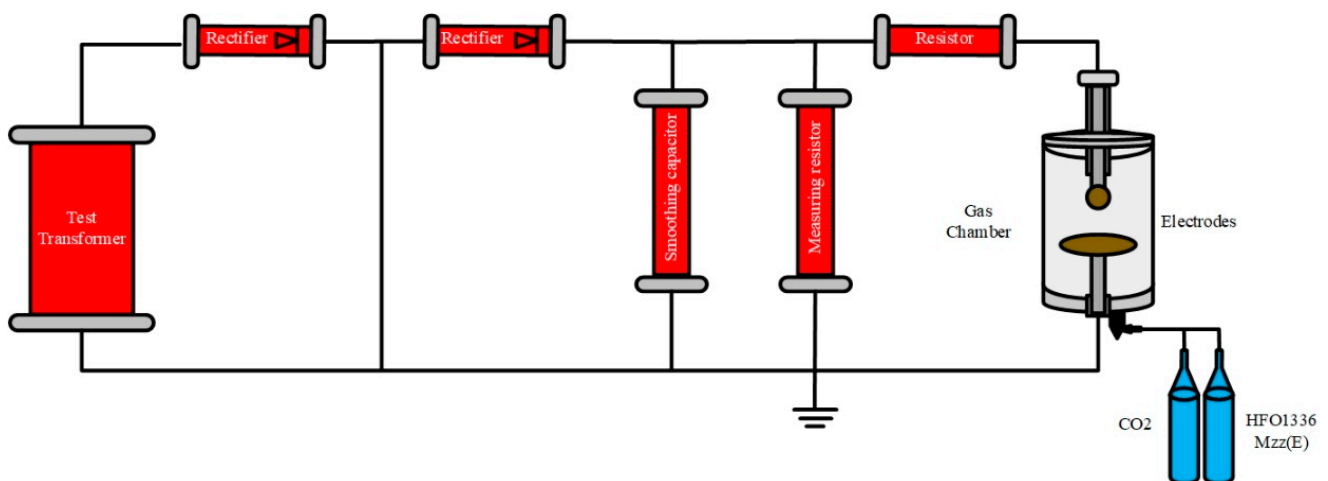


Figure 4. HVDC test setup.

Finite Element Modeling (FEM)

It is difficult to accurately measure the electric field at every point between the electrodes. Additional challenges should be solved since the electrodes are plunged into pressurized gas in a test chamber. A more practical and economical method of carrying out

the measurements is using numerical simulation techniques with computer-aided software. This enables users to skip expensive, intricate, trial-and-error laboratory procedures that are pretty challenging. The electric field utilization factor and field distribution modeling is carried out in this research using the finite element modeling software COMSOL Multiphysics. In FEM software, the geometry of the configuration is constructed, and boundary value conditions are specified [25]. The distribution of the electric field was simulated using the electrostatics module. The analysis necessitates the identification of electrostatic boundary conditions and material properties. An essential element for the simulation is the relative permittivity ϵ_r ; the ϵ_r values of plexiglass and aluminum are 3.4 and 1, respectively, and the gas permittivity value is also selected as 1. The 0 V voltage is at the ground electrode, while the high-voltage electrode is energized with a voltage of 10 V. The bounding box that reflects the real size of the gas chamber is used to symbolize it with dimensions of 140 mm \times 80 mm. Similar to the practical experiments, the air gap between electrodes is fixed at 6 mm. The electric field distribution at each point is precisely calculated with the meshing size set to a user-defined extra fine. The design meshing consists of 15,235 domain elements and 384 boundary elements.

The electric field potential for uniform fields configured by plane–plane electrode configurations is shown in Figure 5. It can be seen that the potential is highest at the HV electrode surface and decreases gradually until 0 V at the ground electrode.

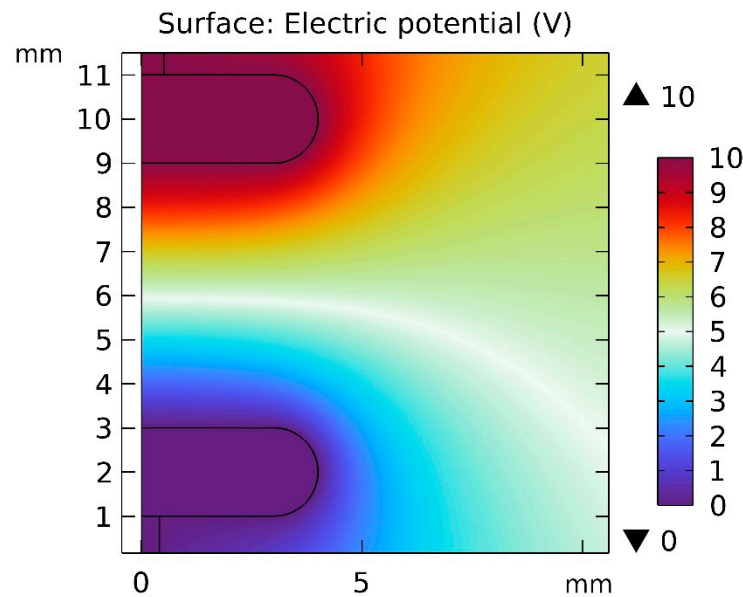


Figure 5. Electric potential simulation of electrodes in a uniform field.

When the boundary conditions are satisfied, calculating the electrostatic field requires Gauss’s and Poisson’s equations. The equations are stated as

$$E = -\nabla V \tag{1}$$

$$\nabla V = -\frac{\rho}{\epsilon_0} \tag{2}$$

Here E represents the electric field, the applied voltage is represented by V , ρ shows space charge density, and ϵ_0 represents the dielectric permittivity of free space.

The law of charge conservation must be obeyed by the electric field strength:

$$\nabla \cdot j = 0 \tag{3}$$

$$j = \rho \cdot v = \rho \cdot \mu \cdot E \tag{4}$$

Here v represents the drift velocity and μ represents the ion mobility across electrode gap distance, by the following equation:

$$\nabla \left\{ \left(\nabla^2 V \right) (\nabla V) \right\} = 0 \tag{5}$$

The FEA software ascertains the behavior of the electric field. The E_{max} and field utilization factor η for each electrode layout were assessed using the breakdown information from the experimental testing. For the sphere–plane and plane–plane configurations, Figures 6 and 7 illustrate that the E_{max} occurs in a location of extremely high stress, which measures 1.7475 V/mm on a sphere–plane system and 2.24986 V/mm on a plane–plane system. FEA simulation aims to gather more information about the electric field distribution at every step, which is impossible to observe during practical experiments. As seen in Figures 6 and 7, the sphere–sphere electrode configuration reveals a higher stress point at the center of the electrodes, and the plane–plane electrode configuration shows the highest electric field point at the side edge of the electrode. The field utilization factor η is calculated using Equation (6).

$$\eta = E_{mean}/E_{max} \tag{6}$$

while E_{max} represents the maximum electric field and E_{mean} can be calculated for each electrode configuration as Equation (7) below:

$$E_{mean} = v/d \tag{7}$$

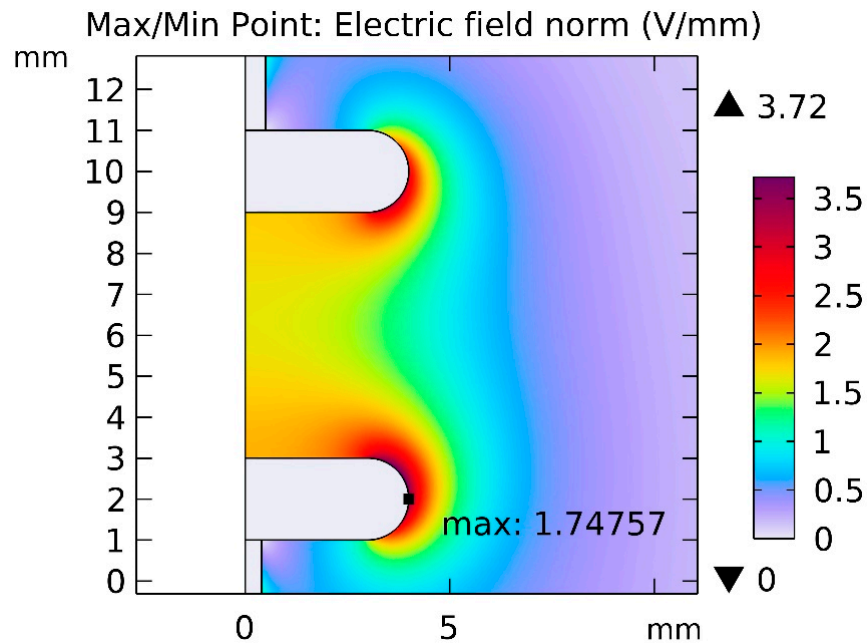


Figure 6. Electric field intensity of plane–plane electrode configuration (uniform field).

Here v represents the applied voltage, and d represents the air gap length between the electrodes. To calculate the utilization factor η , a voltage of 10 v is applied to the high-voltage electrode and the ground electrode is assigned 0 volts. The gap distance is maintained at 6 mm for both configurations. The non-uniform electric field contributes to a higher E_{max} value, and hence lower breakdown voltages. Theoretically, a higher field utilization factor increases the breakdown voltage value. The simulation results presented in this work have field utilization factors for slightly uniform (sphere–plane) and uniform (plane–plane) configurations, which are 0.74 and 0.95, respectively, proving the electric field uniformity of plane electrodes, as shown in Table 2.

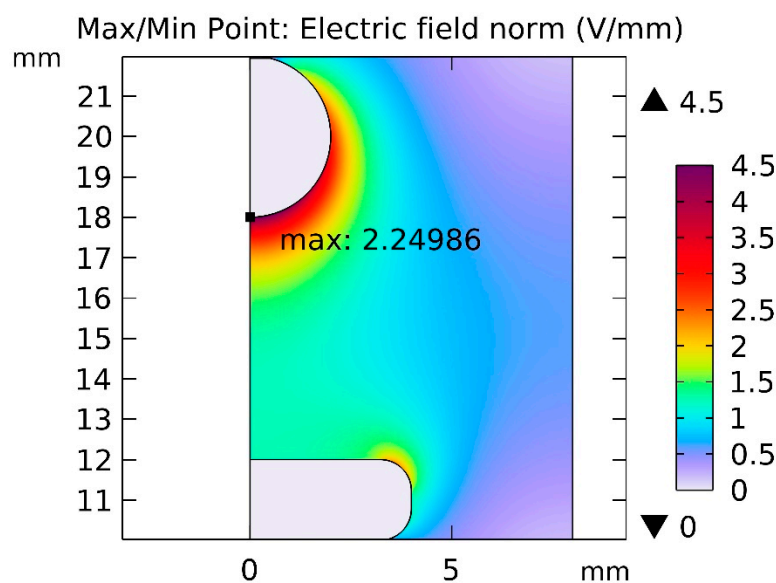


Figure 7. Electric field intensity of sphere–plane electrode configuration (weakly non-uniform field).

Table 2. Electric field utilization factor calculation.

Electrode Configuration	Electric Field Utilization Factor η at Constant 6 mm Air Gap	Electric Field Homogeneity Factor α
Sphere–plane	0.74	1.34
Plane–plane	0.95	1.04

The electrode configuration proposed has a uniform and quasi-uniform electric field; this transition can be analyzed through field inhomogeneity factor α calculation using Equation (8).

$$\alpha = \frac{E_{max}}{E_{mean}} \quad (8)$$

The electric field inhomogeneity factor provides a quantitative measure of how uniform the electric field is within a specified region or across specific boundaries. This factor quantifies how much the electric field deviates from uniformity. If α is close to zero, it indicates that the electric field is nearly uniform. Conversely, as α increases, it signifies a more significant deviation from uniformity, indicating a more inhomogeneous electric field.

4. Experimental Results

Experimental results were obtained by varying pressure from 0.05 to 0.30 MPa and increasing the mixing ratio from 10–30% of base gas and 70–90% of buffer gas. The pressure is varied to determine the gas mixture characterization for medium- or high-voltage switchgear. Based on the results, it is evident that the proposed gas mixture can be utilized for a medium-voltage switchgear system, as it shows promising results at pressure 0.20 MPa or below. The mixing values are varied to determine the optimum mixing ratio, which can be employed in practical applications with dielectric strength comparable to the benchmark SF₆ gas. The insulation performance reliability of the HFO1336Mzz (E)/CO₂ gas mixtures is assessed by comparing with the benchmark SF₆. SF₆ gas is tested along with all the proposed test gas mixture combinations under the same testing conditions and field configurations. In sphere–plane configuration under AC test voltage of 30%, the base gas mixture at 0.15 MPa shows 1.2 times higher dielectric strength than SF₆.

Similarly, the proposed mixture shows 0.9 times dielectric strength for DC voltage compared to SF₆. On the other hand, plane–plane configuration under AC voltage shows

1.60 times and under DC voltage shows 1.15 times higher breakdown strength than SF₆. The detailed experimental results under HVAC and HVDC are discussed in Section 4.1.

4.1. HVAC Breakdown Characteristics of HFO-1336mzz (E) Mixture with CO₂/N₂ under Quasi-Uniform Electric Field

The HVAC dielectric properties of the test mixtures are comprehensively investigated in terms of breakdown voltages relative to absolute pressure and mixing ratios. The HVAC breakdown properties of the HFO-1336mzz (E)/CO₂ and HFO-1336mzz (E)/N₂ mixtures are investigated under uniform and weakly uniform electric field configurations. HFO-1336mzz (E) has a high liquefaction temperature of 7.5 °C, so it needs to be mixed with buffer gases such as CO₂ and N₂. The buffer gases N₂/CO₂ are inert in nature; hence, they de-energize free electrons and help reduce the overall greenhouse gas effect. It is evident from Figure 8a that breakdown voltages of the HFO-1336mzz (E)/CO₂ gas mixture significantly increase with the increase in applied pressure and mixing ratio. It is because of the significant electro-negativity properties of the proposed gas and the positive synergistic effect between the base gas and buffer gas. Under a quasi-uniform field configuration (sphere–Plane), the breakdown voltages increase nonlinearly with increasing pressure. It is observed that when the HFO-1336mzz (E) mixing ratio is 20% or more, it has a higher breakdown voltage than SF₆ at a pressure of less than 0.2 MPa. When the pressure increases from 0.2 MPa, the HFO-1336mzz (E)’s breakdown voltage decreases compared to SF₆. At 0.1 MPa and increasing the base gas mixing ratio from 10 to 30%, the proposed gas breakdown potential increases from 10.5 to 22.4 kV. When the HFO-1336mzz (E) mixing ratio is 20%, the breakdown increases from 17.6 kV to 29.7 kV from a pressure of 0.05 to 0.3 MPa. When pressure increases from 0.2 MPa, the proposed gas mixture breakdown voltage is less than SF₆, i.e., at 0.3 bar, SF₆’s breakdown strength is 1.17 times higher than that of HFO-1336mzz (E)/CO₂. In addition, by increasing the gas content of HFO-1336mzz (E) in the gas mixture, the breakdown voltage also increases relatively. When the mixing ratio of HFO-1336mzz (E) is 30%, at 0.15 MPa, the breakdown strength is 1.4 times higher than that of SF₆. A similar effect can be seen for HFO-1336mzz (E)/N₂ mixtures, in which the highest breakdown strength is achieved when the base gas mixing ratio is the maximum, i.e., 30%. The HFO-1336mzz (E)/N₂ mixture’s initial breakdown voltages at lower pressure, i.e., 0.05 and 0.1 MPa, have a 0.67 percent lower breakdown value than the CO₂ mixture. HFO-1336mzz (E)/N₂ mixtures show relatively nonlinear results as compared to HFO-1336mzz (E)/CO₂. However, in both cases, the proposed gas mixtures show superior insulation properties at 0.15–0.20 MPa pressure, as seen in Figure 8.

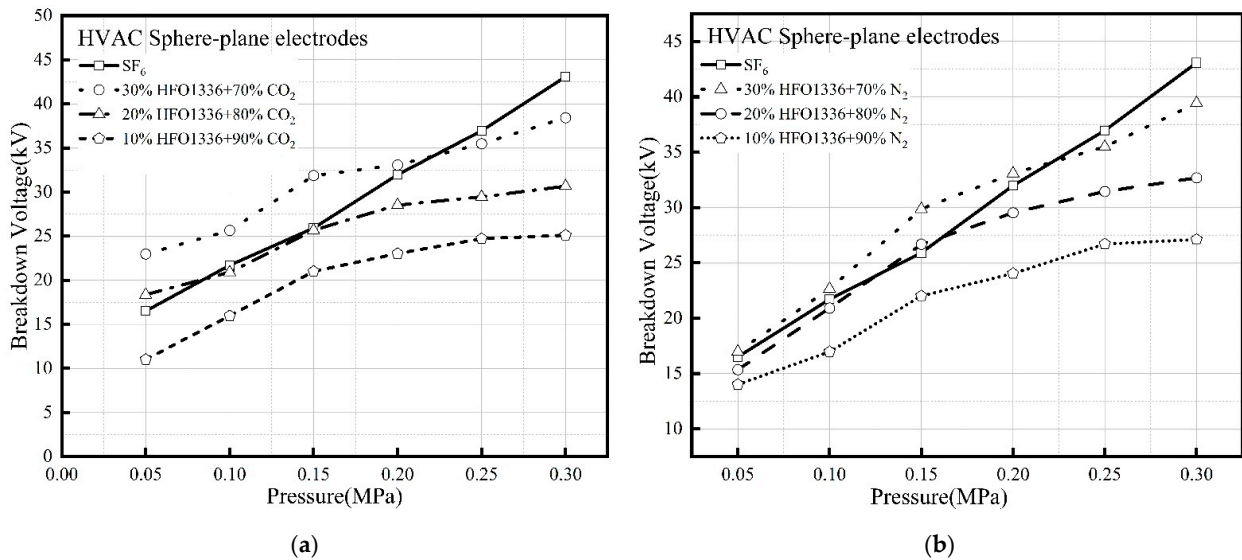


Figure 8. Breakdown voltages of (a) HFO-1336mzz (E)/CO₂ and (b) HFO-1336mzz (E)/N₂ at quasi-uniform field.

4.2. HVAC Breakdown Characteristics of HFO-1336mzz (E) Mixture with CO₂/N₂ under Uniform Electric Field

HFO-1336mzz (E)/CO₂ and HFO-1336mzz (E)/N₂ mixtures have increased dielectric strength values when pressure and mixing ratio increase. Similarly, the breakdown properties of HFO-1336mzz (E)/CO₂ under HVAC test conditions are investigated for uniform field configurations of plane–plane electrodes, as shown in Figure 8b. Linearity in the breakdown voltage curve is observed in uniform field configuration with increasing pressure. It can be noted that the 30% base gas mixture under the uniform electric field shows an approximately 1.04 times higher breakdown voltage than SF₆ at a 0.6 mm constant air gap for all applied pressure ranges. The results for the N₂ mixture under the same test configuration reveal that the 30% base gas mixture above 0.15 mixture has a higher dielectric breakdown voltage value than SF₆. Below 0.15 MPa voltage, all N₂ mixtures have lower breakdown values, as can be seen in Figure 9.

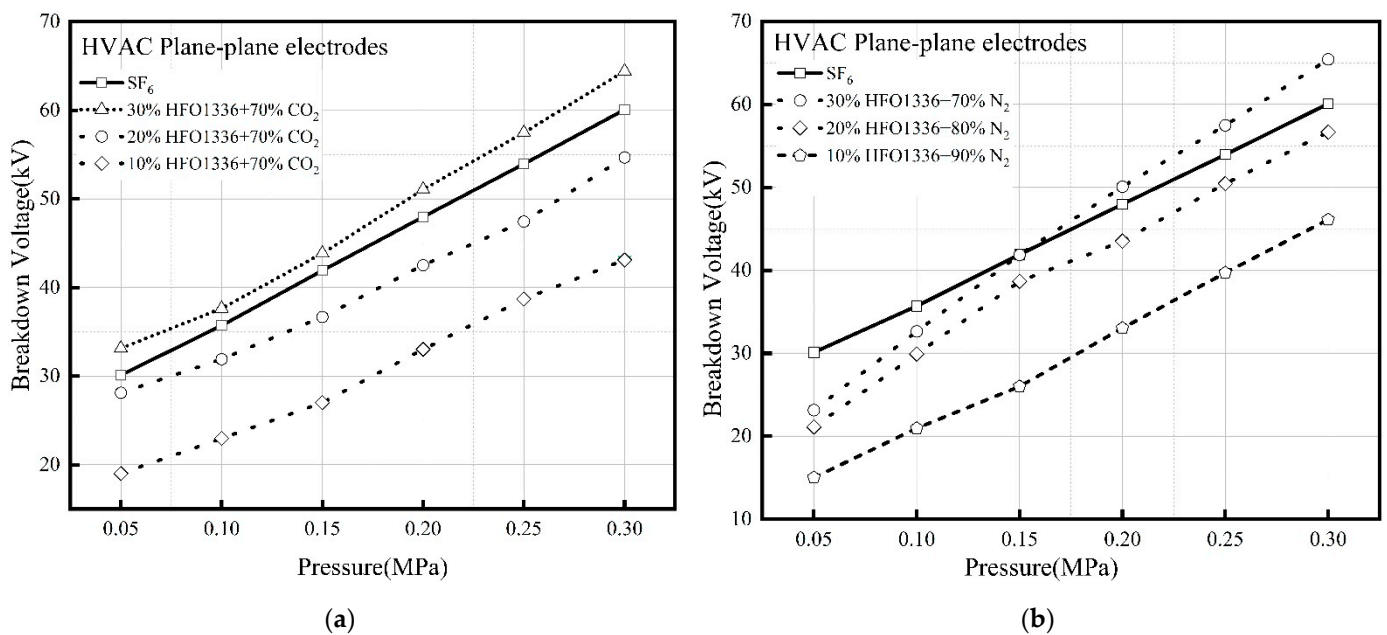


Figure 9. Breakdown voltages of (a) HFO-1336mzz (E)/CO₂ and (b) HFO-1336mzz (E)/N₂ at uniform field.

4.3. HVDC Breakdown Characteristics of HFO-1336mzz (E) Mixture with CO₂/N₂ under Quasi-Uniform Electric Field

DC breakdown experiments were performed at 0.05–0.3 MPa to examine the impact of the mixing ratio on the breakdown strength of the HFO-1336mzz (E) mixtures. The findings are displayed in Figure 10. With a rise in HFO-1336mzz (E) gas concentration, the proposed gas mixture’s breakdown voltages grow nonlinearly, showing the proposed gas’s sensitivity to the applied electric field. In sphere–plane electrode configuration, the 30% HFO-1336mzz (E)/CO₂ gas mixture shows nearly equivalent dielectric strength to SF₆ at 0.2 MPa and HFO-1336mzz (E)/N₂ at 0.1 MPa. SF₆’s breakdown voltage increases linearly with increasing pressure. Under HVDC applied voltage, it is evident that the 30% HFO-1336mzz (E)/CO₂ mixture shows promising results when the pressure applied is below 0.20 MPa. When pressure is increased from 0.2 MPa, the breakdown voltage of SF₆ continues to increase, but the gas mixture under test shows a decreasing trend, specifically for the N₂ mixture. It reveals the stable insulation properties of SF₆ and enhanced dielectric properties of the CO₂ mixture at lower pressure. Both of the proposed buffer gas mixtures at a pressure above 0.25 MPa show nonlinearity in breakdown voltage, which is due to the same polarity effect of DC, along with the fact that the electrodes’ surface state and area

may be the driving nonlinearity factors at higher pressure values. At pressure values below 0.15 MPa, the values are relatively linear.

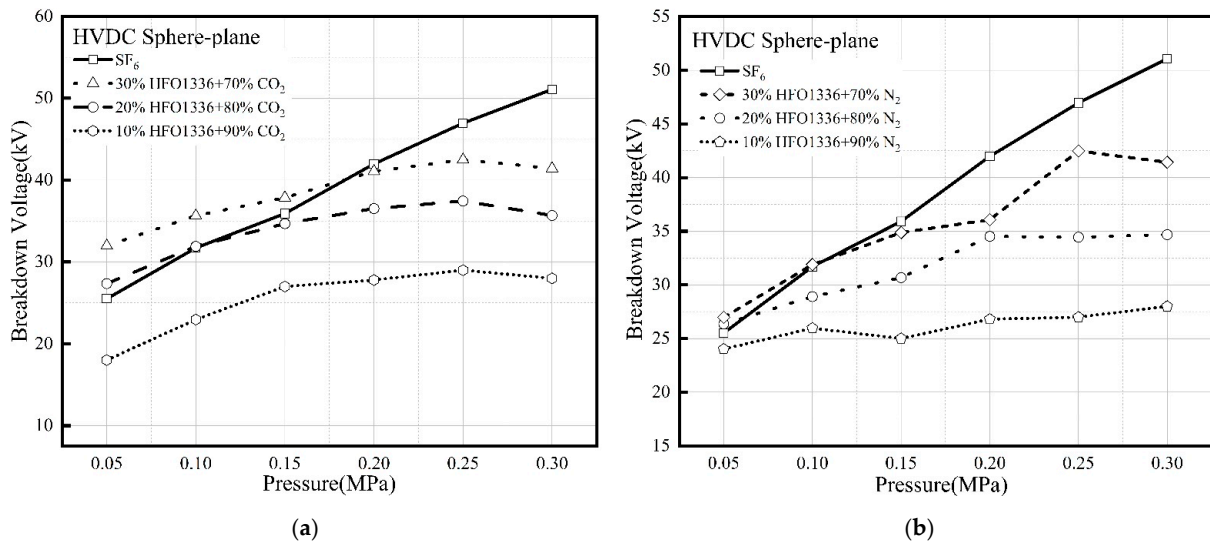


Figure 10. Breakdown voltages of (a) HFO-1336mzz (E)/CO₂ and (b) HFO-1336mzz (E)N₂ at quasi-uniform field.

4.4. HVDC Breakdown Characteristics of HFO-1336mzz (E) Mixture with CO₂/N₂ under Uniform Electric Field

Similarly, the HVDC breakdown properties of the proposed mixture are investigated under uniform field configuration. It is evident that the breakdown strength of the test gas increases linearly with an increase in pressure and mixing ratio. Nevertheless, the 30% HFO-1336mzz (E)/CO₂ has 1.21 times higher dielectric strength than SF₆ at 0.15 MPa under uniform field configuration, as can be seen in Figure 11a. The 30% base gas concentration shows a more promising result in terms of dielectric strength than SF₆. The 30% base gas mixture composition can be used for medium-voltage applications. The dielectric characteristics of HFO-1336mzz (E)/N₂ for the uniform field configuration can be seen in Figure 11b. SF₆ shows a linear increase in breakdown voltage, and nonlinearity can be seen in the proposed gas mixture. The 30% HFO-1336mzz (E)/N₂ mixture at lower pressure of less than 0.23 MPa shows lower breakdown strength, but higher than SF₆. Above 0.23 MPa, the breakdown voltage increases with respect to SF₆. The 30% HFO-1336mzz (E)/N₂ mixture at 0.30 MPa pressure reveals 1.06 times higher breakdown voltage value than SF₆.

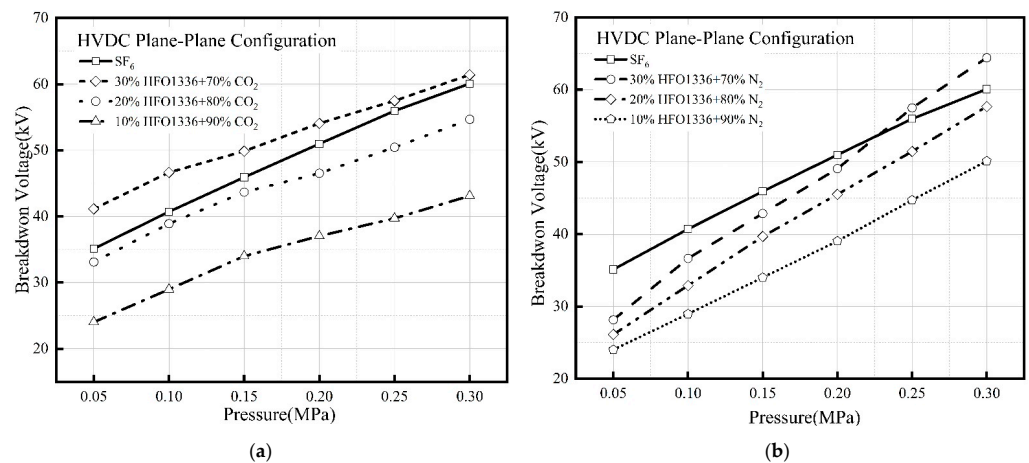


Figure 11. Breakdown voltages of (a) HFO-1336mzz (E)/CO₂ and (b) HFO-1336mzz (E)N₂ at uniform field.

5. Other Characterization of the Dielectric Gas Mixture

5.1. Global Warming Potential of HFO-1336mzz (E)/CO₂ Gas Mixture

The global warming potential of HFO-1336mzz (E) is 18, which is considerably less than SF₆. The proposed gas mixture has been developed as an alternative to SF₆, but the GWP of the mixture needs to be investigated. According to the environmental protection view and ideal gas conditions, the GWP is determined by summing the weight fractions of each component and multiplying that number by their respective GWP, as shown in Equation (9) [24,26]. k represents the mixing ratio of base gas, and the GWP and molar mass of HFO-1336mzz (E) are 18 and 164.5, respectively. Similarly, the GWP and molar mass of CO₂ are 1 and 44, respectively. The mixing ratio of the base gas is increased from 1 to 100%, and the GWP value also starts increasing from 1 to 18. It is evident from the results presented in Figure 12 that the proposed mixture has a negligible environmental concern compared to SF₆, which has 23,500 GWP.

$$\text{GWP} = \frac{k \times 164.5 \times 18 + (1 - k) \times 44 \times 1}{k \times 164.5 + (1 - k) \times 44} \quad (9)$$

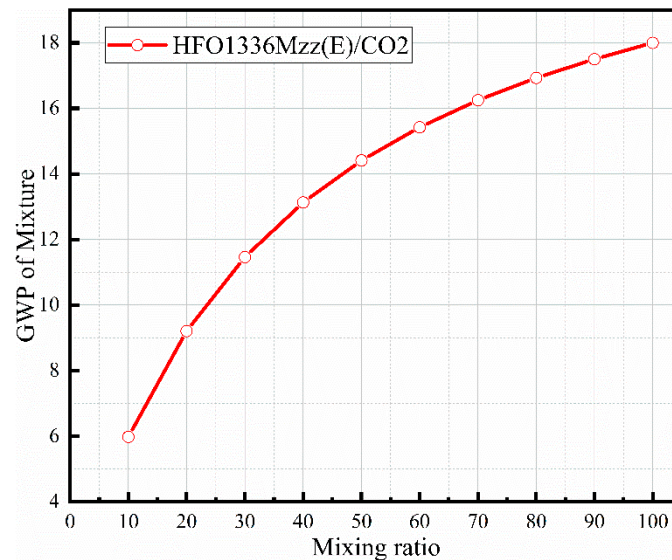


Figure 12. GWP of HFO-1336mzz (E)/CO₂ mixture.

5.2. Liquefaction Temperature

The important parameter for a dielectric gas is its liquefaction temperature, which is applicable in practical applications. The liquefaction temperature is the point at which gases melt to a liquid state. At high pressure, the temperature of dielectric gas also increases, transforming the gaseous state to a liquid. The HFO-1336mzz (E) boiling point is comparatively high, at 7.58 °C at 0.1 MPa pressure; hence, it cannot be employed for low-temperature applications. Therefore, it is mixed with buffer gases such as CO₂ and N₂, having low liquefaction temperatures of −79 °C and −196 °C, respectively, at 0.1 MPa pressure. The HFO-1336mzz (E) and CO₂ mixture's liquefaction temperatures are analyzed. The relationship between the liquefaction temperature at room conditions T_b , vapor pressure (P), and liquefaction temperature of the base gas in mixture T is expressed in Equation (10). A and R are gas constants with values of 87 J/mol. K and 8.3 J/mol. K, respectively.

$$P = \exp \left[\frac{A}{R} \left(1 - \frac{T_b}{T} \right) \right] \quad (10)$$

Equation (11) can be modified by introducing m , a mixing ratio, by considering ideal gas conditions; the HFO-1336mzz (E) and CO₂ mixture’s liquefaction temperature can be calculated using Equation (5) [27].

$$T_{mb} = \frac{T_b}{1 - \frac{\ln(10mP)}{A/R}} \tag{11}$$

The HFO-1336mzz (E) and CO₂ mixture’s liquefaction temperatures with different mixing ratios and pressure ranges, from 0.1 to 0.3 MPa, are depicted in Figure 13. Increasing the pressure and the HFO-1336mzz (E) percentage in the mixture increases the liquefaction temperature. A similar relation is observed by increasing the pressure, which increases the liquefaction temperature. Figure 13 indicates the constraint on the choice of mixing ratio and pressure. If, for instance, a pressure of 0.1 MPa and a critical temperature of −20 °C are required for medium-voltage application, the HFO-1336mzz (E) mixing ratio should not exceed 30%. Similarly, for 0.2 and 0.3 MPa, the HFO-1336mzz (E) should be within 15% and 10%, respectively.

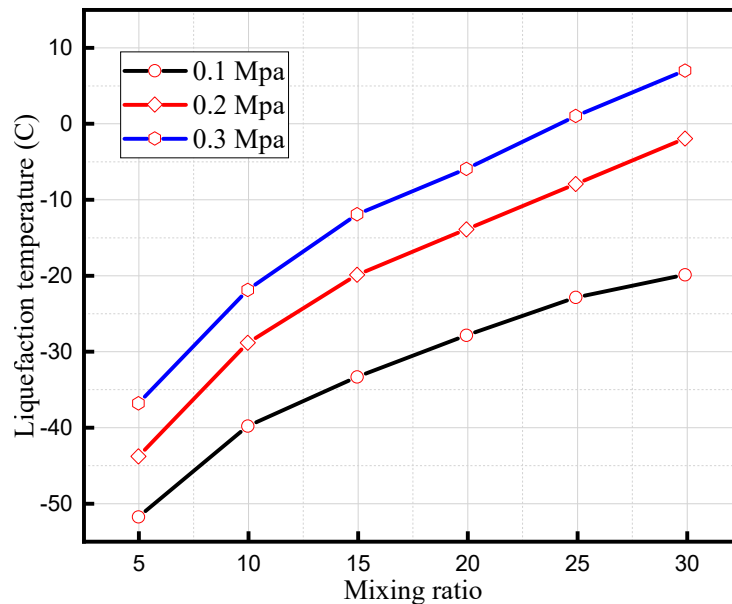


Figure 13. Liquefaction temperature of HFO-1336mzz (E)/CO₂.

5.3. Synergistic Effect of HFO-1336mzz (E)

The synergistic effect characterizes the gas mixture’s dielectric strength, as mixing two gases results in higher or lower breakdown voltages than in their pure form. To analyze the synergistic effect of the HFO-1336mzz (E)/CO₂ gas mixture, a coefficient S is introduced, as can be seen in Equation (12) [28]. In the equation, V_{buffer} , V_{base} , and V_{mix} show CO₂ breakdown voltage, HFO-1336mzz (E), and their mixture, where m denotes the percentage mixture of HFO-1336mzz (E) in the gas mixture.

$$V_{mix} = V_{buffer} + \frac{m(V_{base} - V_{buffer})}{m + (1 - m)S} \tag{12}$$

$$V_{base} > V_{buffer}$$

Figure 14 shows the synergistic effect of HFO-1336mzz (E) with CO₂ gas. If $S = 0$, it means there is no synergistic effect, i.e., the breakdown of the mixture is equal to a weighted sum of the component gases and shows a linear effect of V_{mix} with m . If $S > 0$, it means the gas mixture weighted average is greater than the component gases and is known as a negative synergistic effect. If $S < 0$, it means the gas mixture weighted sum is less than the

component gases and is known as the positive synergistic effect. If $0 < S < 1$, it shows a synergistic effect.

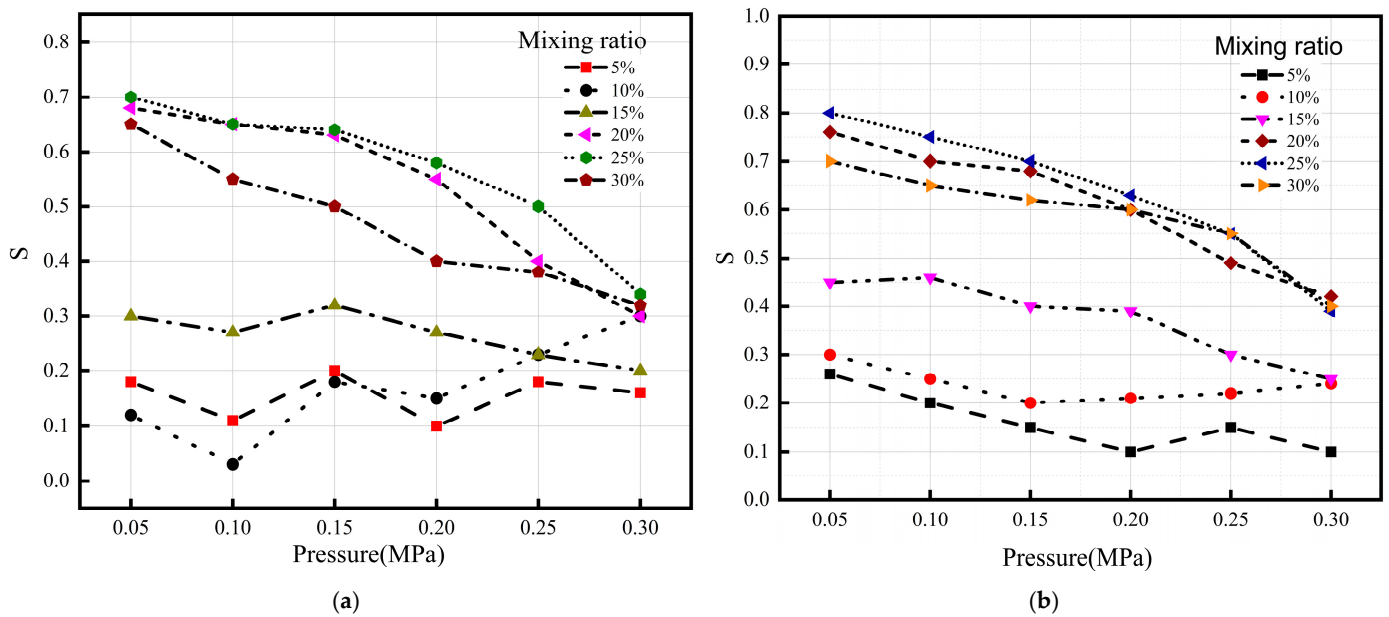


Figure 14. Synergistic effect of (a) HFO-1336mzz (E)/CO₂ gas mixture and (b) HFO-1336mzz (E)/N₂ gas mixture.

Figure 14 above shows the S value for HFO1336Mzz (E)/CO₂ and HFO1336Mzz (E)/N₂ for pressure ranges from 0.05 to 0.3 MPa and a mixing ratio ranging from 70 to 90% of base gas proportion in the gas mixture. It is evident from the figure that for all mixture compositions, the S values for HFO1336Mzz (E)/CO₂ are lower than HFO1336Mzz (E)/N₂. In the case of HFO1336Mzz (E)/CO₂, the mixture composition of (90/10%) for all pressure ranges shows the S coefficient value close to zero, indicating a positive synergistic effect. Moreover, the HFO1336Mzz (E)/CO₂ S values are 0 to 0.7, while the HFO1336Mzz (E)/N₂ values range from 0 to 0.8.

Therefore, even though the two types of buffer gases have almost equivalent dielectric strength, the dielectric breakdown strength of HFO1336Mzz (E)/N₂ is inferior to HFO1336Mzz (E)/CO₂ mixtures, as validated through synergistic effect analysis.

5.4. Self-Recoverability Test

Self-recoverability of insulation is the ability of insulation to restore itself after breakdown caused by temperature rise and overvoltage. The self-recoverability of gas is tested by analyzing the consecutive AC breakdown voltages at 3 min. A total of 40 breakdown shots were recorded, and it was found that the 70%CO₂/30%HFO-1336mzz (E) mixture shows a little deviation from the initial breakdown at around 30 shots. After the 30th breakdown, the voltage shows a decreasing trend, but the percentage difference between the first and last breakdown is still as low as 5%. It is due to the decomposition of the mixture and ionization of gas particles, which are conductive in nature and reduce the breakdown voltages. Another reason might be the conductive carbon deposition on the surface of the electrodes. Hence, the experiment concluded that the 70%CO₂/30%HFO-1336mzz (E) mixture could be successfully employed for high-voltage applications at higher pressure. In Figure 15, the self-recoverability of the gas mixture is plotted.

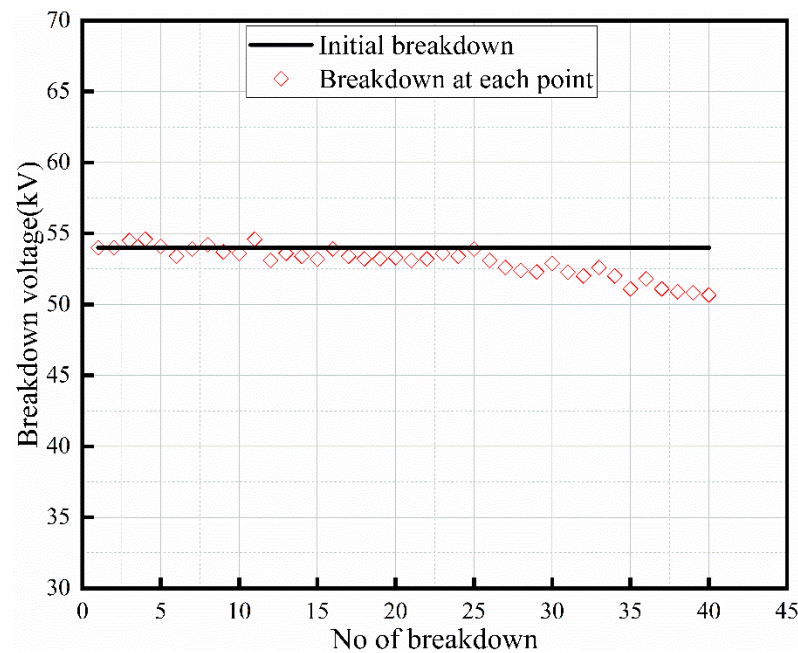


Figure 15. Self-recoverability of HFO-1336mzz (E)/CO₂ mixture.

6. Conclusions

This paper has systematically investigated HVAC and HVDC voltage breakdown characteristics of HFO-1336mzz (E) mixed with CO₂/N₂ as an environmentally friendly alternative for gas-insulated applications. The mixture ratio and gas pressure influence on the insulation characteristics of the proposed gas mixture are investigated under uniform (plane–plane) and quasi-uniform (sphere–plane) electric fields and compared with the hazardous SF₆ gas. Finite element analysis is performed on HFO-1336mzz (E)/CO₂ to study the electric field distribution of electric potential. The field utilization factor and maximum field intensity point are determined for uniform and weakly non-uniform electric fields. The FEM results reveal a uniform electric field in plane–plane configuration comparable to experimental results. Experimental results show that under quasi-uniform electric fields, the 30% HFO-1336mzz (E) at a pressure below 0.2 MPa has relative HVAC and HVDC dielectric strength equivalent to SF₆. Under uniform field configuration at 0.3 MPa, the gas mixture’s AC and DC dielectric strength is comparable to SF₆. Furthermore, a synergistic effect of the proposed gas mixture shows favorable results, as synergistic coefficient *S* values between HFO-1336mzz (E) and CO₂ are in the range of 0.05–0.75. The GWP potential of the test mixture for all the mixing ratios is calculated, and it is found that the maximum GWP value is 18, which proves the claim of an eco-friendly alternative to SF₆. Additionally, the self-recoverability testing of the 30% HFO-1336mzz (E) + 70% CO₂ mixture reveals that after 40 consecutive breakdowns shots, only a 5% minimum difference is noted between the first and last breakdown. The 30% HFO-1336mzz (E)/CO₂ gas mixture at 0.15–0.20 MPa pressure and constant 0.6 mm air gap in relevance to practical MV-GIE reveals superior insulation tolerance and less sensitivity to the electric field brings about its potential engineering applications.

Author Contributions: Conceptualization, R.A.R. and R.A.; methodology, R.A.; software, R.A. and A.J.; validation, R.A.; formal analysis, A.S.A., B.A.-R. and A.J.; investigation, R.A. and R.U.; resources, R.U.; data curation, R.A.; writing—original draft preparation, R.A.; writing—review and editing, R.A., A.J. and R.U.; visualization, B.A.-R. and A.S.A.; supervision, R.A.R.; project administration, A.S.A., A.J. and R.U.; funding acquisition, R.A.R., A.S.A. and B.A.-R. All authors have read and agreed to the published version of the manuscript.

Funding: This research received no external funding.

Institutional Review Board Statement: Not applicable.

Informed Consent Statement: Not applicable.

Data Availability Statement: Not applicable.

Acknowledgments: This research was supported by The Ministry of Higher Education (MOHE) Malaysia through the Fundamental Research Grant Scheme (FRGS/1/2020/TKO/UTHM/02/6), and we acknowledge the support of King Fahd University of Petroleum & Minerals.

Conflicts of Interest: The authors declare no conflict of interest.

Abbreviation

HFO	Hydrofluoroolefins
ODP	Ozone Depletion Potential
SF ₆	Sulfur Hexafluoride
HV	High Voltage
CO ₂	Carbon Dioxide
GWP	Global Warming Potential
HVAC	High-Voltage Alternating Current
HVDC	High-Voltage Direct Current
IEC	International Electro Technical Commission
FEM	Finite Element Modelling
GND	Ground
kV	Kilovolt

References

- Mohamed, R.; Christian, M.F. Assessment of eco-friendly gases for electrical insulation to replace the most potent industrial greenhouse gas SF₆. *Environ. Sci. Technol.* **2018**, *52*, 369–380.
- Christophorou, L.G.; Olthoff, J.K.; Brunt, R.J.V. Sulfur hexafluoride and the electric power industry. *IEEE Electr. Insul. Mag.* **1997**, *13*, 20–24. [[CrossRef](#)]
- Simmonds, P.G.; Rigby, M.; Manning, A.J.; Park, S.; Stanley, K.M.; McCulloch, A.; Stephan, H.; Prinn, R.G. The increasing atmospheric burden of the greenhouse gas sulfur hexafluoride (SF₆). *Atmos. Chem. Phys.* **2020**, *20*, 7271–7290. [[CrossRef](#)]
- IPCC. *Climate Change 2013: The Physical Science Basis. Working Group I Contribution to the Fifth Assessment Report on Intergovernmental Panel on Climate Change*; Cambridge University Press: Cambridge, UK, 2013.
- U.S. Environmental Protection Agency (USEPA). *Global Mitigation of Non-CO₂ Greenhouse Gases: 2010–2030*; USEPA: Washington, DC, USA, 2013.
- Breidenich, C.; Magraw, D.; Rowley, A.; Rubin, J.W. The Kyoto protocol to the United Nations framework convention on climate change. *Am. J. Int. Law* **1998**, *92*, 315–331. [[CrossRef](#)]
- Beroual, A.; Haddad, A. Recent advances in the quest for a new insulation gas with a low impact on the environment to replace sulfur hexafluoride (SF₆) gas in high-voltage power network applications. *Energies* **2017**, *10*, 1216. [[CrossRef](#)]
- Khan, B.; Saleem, J.; Khan, F.; Faraz, G.; Ahmad, R.; Ur Rehman, N.; Ahmad, Z. Analysis of the dielectric properties of R410A Gas as an alternative to SF₆ for high, & Ahma applications. *High Volt.* **2019**, *4*, 41–48.
- Abd-Rahman, R.; Haddad, A.; Kamarudin, M.S.; Yousof, M.F.M.; Jamail, N.A.M. Dynamic modelling of polluted outdoor insulator under wet weather conditions. In Proceedings of the PECON 2016—2016 IEEE 6th International Conference on Power and Energy, Conference Proceeding, Melaka, Malaysia, 28–29 November 2016; pp. 610–614.
- Owens, J.G. Greenhouse gas emission reductions through use of a sustainable alternative to SF₆. In Proceedings of the 2016 IEEE Electrical Insulation Conference (EIC), Montreal, QC, Canada, 19–22 June 2016; IEEE: New York, NY, USA, 2016; pp. 535–538.
- Ahmed, R.; Abd Rahman, R.; Kamarudin, M.S.; Yousof, M.F.M.; binti Ahmad, H.; Salem, A.A. Feasibility of Fluoronitrile (C₄F₇N) as a Substitute to Sulphur Hexafluoride (SF₆) in Gas Insulated Application: A Review. In Proceedings of the 2022 IEEE International Conference on Power and Energy (PECon), Langkawi, Malaysia, 5–6 December 2022; IEEE: New York, NY, USA, 2022; pp. 391–396.
- Ahmad, R.; Abd Rahman, R.; Salem, A.A.; Jamail, N.A.M.; Ab Rahman, A.; Hamid, H.A. Finite Element Analysis of Electric Field Distribution in C₄F₇N as an Alternative to SF₆ For Electrical Insulation. In Proceedings of the 2021 3rd International Conference on High Voltage Engineering and Power Systems (ICHVEPS), Bandung, Indonesia, 5–6 October 2021; IEEE: New York, NY, USA, 2021; pp. 126–131.
- Xiao, S.; Tian, S.; Zhang, X.; Cressault, Y.; Tang, J.; Deng, Z.; Li, Y. The influence of O₂ on decomposition characteristics of c-C₄F₈/N₂ environmental friendly insulating gas. *Processes* **2018**, *6*, 174. [[CrossRef](#)]

14. Tan, D.; Zhou, B.; Xue, J.; Cai, F.; Xiao, D. Basic impulse performance of high-pressure CF_3IN_2 gas mixture and its application for 126 kV GIL. *IEEE Trans. Dielectr. Electr. Insul.* **2018**, *25*, 1380–1386.
15. Chen, L.; Widger, P.; Kamarudin, M.S.; Griffiths, H.; Haddad, A. CF_3I gas mixtures: Breakdown characteristics and potential for electrical insulation. *IEEE Trans. Power Deliv.* **2016**, *32*, 1089–1097. [[CrossRef](#)]
16. Wang, X.; Wang, Z.; Chen, J.; Shi, X.; Li, X. Surface Flashover Characteristics of Epoxy Resin Composites in SF_6/CF_4 Gas Mixture with DC Voltage. *Energies* **2022**, *15*, 4675. [[CrossRef](#)]
17. Koch, M.; Franck, C.M. High voltage insulation properties of HFO1234ze. *IEEE Trans. Dielectr. Electr. Insul.* **2015**, *22*, 3260–3268. [[CrossRef](#)]
18. Yokomizu, Y.; Sato, M.; Kodama, N.; Edo, T.; Kokura, K. Chemical species produced in arc-quenching gas CO_2/O_2 mixed with $\text{C}_3\text{H}_2\text{F}_4$, $\text{C}_4\text{-FN}$ or $\text{C}_5\text{-FK}$: Prevention of condensed-phase carbon formation and its formulation. *J. Phys. D Appl. Phys.* **2020**, *53*, 145202. [[CrossRef](#)]
19. Li, Y.; Zhang, X.; Xiao, S.; Chen, Q.; Tang, J.; Chen, D.; Wang, D. Decomposition properties of $\text{C}_4\text{F}_7\text{N}/\text{N}_2$ gas mixture: An environmentally friendly gas to replace SF_6 . *Ind. Eng. Chem. Res.* **2018**, *57*, 5173–5182. [[CrossRef](#)]
20. Abd Rahman, R.; Harid, N.; Haddad, A. Stress control on polymeric outdoor insulators. In Proceedings of the 45th International Universities Power Engineering Conference UPEC2010, Cardiff, UK, 31 August–3 September 2010; IEEE: New York, NY, USA, 2010; pp. 1–4.
21. Huo, E.; Liu, C.; Xin, L.; Li, X.; Xu, X.; Li, Q.; Wang, S.; Dang, C. Thermal stability and decomposition mechanism of HFO-1336mzz (Z) as an environmental friendly working fluid: Experimental and theoretical study. *Int. J. Energy Res.* **2019**, *3*, 4630–4643. [[CrossRef](#)]
22. Rabie, M.; Franck, C.M. Computational screening of new high voltage insulation gases with low global warming potential. *IEEE Trans. Dielectr. Electr. Insul.* **2015**, *22*, 296–302. [[CrossRef](#)]
23. Kothe, D.C.; Hinrichsen, V.; Ermeler, K.; Kalter, A. Experimental investigation of dielectric properties of alternative insulation gases for medium voltage switchgear. In Proceedings of the VDE High Voltage Technology 2020; ETG-Symposium, Online, 9–11 November 2022; VDE: Berlin, Germany, 2022; pp. 1–6.
24. Zhang, B.; Chen, L.; Li, X.; Guo, Z.; Pu, Y.; Tang, N. Evaluating the dielectric strength of promising SF_6 alternatives by DFT calculations and DC breakdown tests. *IEEE Trans. Dielectr. Electr. Insul.* **2020**, *27*, 1187–1194. [[CrossRef](#)]
25. IEC-60270; High-Voltage Test Techniques: Partial Discharge Measurements. International Electro Technical Commission: Geneva, Switzerland, 2000; pp. 13–31.
26. D2477-07; Standard Test Method for Dielectric Breakdown Voltage and Dielectric Strength of Insulating Gases at Commercial Power Frequencies. ASTM International: West Conshohocken, PA, USA, 2012.
27. Kharal, H.S.; Kamran, M.; Ullah, R.; Saleem, M.Z.; Alvi, M.J. Environment-friendly and efficient gaseous insulator as a potential alternative to SF_6 . *Processes* **2019**, *7*, 740. [[CrossRef](#)]
28. Salem, A.A.; Abd-Rahman, R.; Kamarudin, M.S.; Ahmed, H.; Jamail, N.A.M.; Othman, N.A.; Yusouf, M.F.M.; Ishak, M.T.; Al-Ameri, S. The effect of insulator geometrical profile on electric field distributions. *Indones. J. Electr. Eng. Comput. Sci.* **2019**, *14*, 618–627. [[CrossRef](#)]

Disclaimer/Publisher’s Note: The statements, opinions and data contained in all publications are solely those of the individual author(s) and contributor(s) and not of MDPI and/or the editor(s). MDPI and/or the editor(s) disclaim responsibility for any injury to people or property resulting from any ideas, methods, instructions or products referred to in the content.